

A Search for $t \rightarrow \tau\nu q$ in $t\bar{t}$ Production

A. Abulencia,²³ D. Acosta,¹⁷ J. Adelman,¹³ T. Affolder,¹⁰ T. Akimoto,⁵³ M.G. Albrow,¹⁶
D. Ambrose,¹⁶ S. Amerio,⁴² D. Amidei,³³ A. Anastassov,⁵⁰ K. Anikeev,¹⁶ A. Annovi,⁴⁴
J. Antos,¹ M. Aoki,⁵³ G. Apollinari,¹⁶ J.-F. Arguin,³² T. Arisawa,⁵⁵ A. Artikov,¹⁴
W. Ashmanskas,¹⁶ A. Attal,⁸ F. Azfar,⁴¹ P. Azzi-Bacchetta,⁴² P. Azzurri,⁴⁴ N. Bacchetta,⁴²
H. Bachacou,²⁸ W. Badgett,¹⁶ A. Barbaro-Galtieri,²⁸ V.E. Barnes,⁴⁶ B.A. Barnett,²⁴
S. Baroiant,⁷ V. Bartsch,³⁰ G. Bauer,³¹ F. Bedeschi,⁴⁴ S. Behari,²⁴ S. Belforte,⁵² G. Bellettini,⁴⁴
J. Bellinger,⁵⁷ A. Belloni,³¹ E. Ben-Haim,¹⁶ D. Benjamin,¹⁵ A. Beretvas,¹⁶ J. Beringer,²⁸
T. Berry,²⁹ A. Bhatti,⁴⁸ M. Binkley,¹⁶ D. Bisello,⁴² M. Bishai,¹⁶ R. E. Blair,² C. Blocker,⁶
K. Bloom,³³ B. Blumenfeld,²⁴ A. Bocci,⁴⁸ A. Bodek,⁴⁷ V. Boisvert,⁴⁷ G. Bolla,⁴⁶ A. Bolshov,³¹
D. Bortoletto,⁴⁶ J. Boudreau,⁴⁵ S. Bourov,¹⁶ A. Boveia,¹⁰ B. Brau,¹⁰ C. Bromberg,³⁴
E. Brubaker,¹³ J. Budagov,¹⁴ H.S. Budd,⁴⁷ S. Budd,²³ K. Burkett,¹⁶ G. Busetto,⁴² P. Bussey,²⁰
K. L. Byrum,² S. Cabrera,¹⁵ M. Campanelli,¹⁹ M. Campbell,³³ F. Canelli,⁸ A. Canepa,⁴⁶
D. Carlsmith,⁵⁷ R. Carosi,⁴⁴ S. Carron,¹⁵ M. Casarsa,⁵² A. Castro,⁵ P. Catastini,⁴⁴ D. Cauz,⁵²
M. Cavalli-Sforza,³ A. Cerri,²⁸ L. Cerrito,⁴¹ S.H. Chang,²⁷ J. Chapman,³³ Y.C. Chen,¹
M. Chertok,⁷ G. Chiarelli,⁴⁴ G. Chlachidze,¹⁴ F. Chlebana,¹⁶ I. Cho,²⁷ K. Cho,²⁷ D. Chokheli,¹⁴
J.P. Chou,²¹ P.H. Chu,²³ S.H. Chuang,⁵⁷ K. Chung,¹² W.H. Chung,⁵⁷ Y.S. Chung,⁴⁷ M. Ciljak,⁴⁴
C.I. Ciobanu,²³ M.A. Ciocci,⁴⁴ A. Clark,¹⁹ D. Clark,⁶ M. Coca,¹⁵ A. Connolly,²⁸ M.E. Convery,⁴⁸
J. Conway,⁷ B. Cooper,³⁰ K. Copic,³³ M. Cordelli,¹⁸ G. Cortiana,⁴² A. Cruz,¹⁷ J. Cuevas,¹¹
R. Culbertson,¹⁶ D. Cyr,⁵⁷ S. DaRonco,⁴² S. D'Auria,²⁰ M. D'onofrio,¹⁹ D. Dagenhart,⁶
P. de Barbaro,⁴⁷ S. De Cecco,⁴⁹ A. Deisher,²⁸ G. De Lentdecker,⁴⁷ M. Dell'Orso,⁴⁴ S. Demers,⁴⁷
L. Demortier,⁴⁸ J. Deng,¹⁵ M. Deninno,⁵ D. De Pedis,⁴⁹ P.F. Derwent,¹⁶ C. Dionisi,⁴⁹
J.R. Dittmann,⁴ P. DiTuro,⁵⁰ C. Dörr,²⁵ A. Dominguez,²⁸ S. Donati,⁴⁴ M. Donega,¹⁹ P. Dong,⁸
J. Donini,⁴² T. Dorigo,⁴² S. Dube,⁵⁰ K. Ebina,⁵⁵ J. Efron,³⁸ J. Ehlers,¹⁹ R. Erbacher,⁷ D. Errede,²³
S. Errede,²³ R. Eusebi,⁴⁷ H.C. Fang,²⁸ S. Farrington,²⁹ I. Fedorko,⁴⁴ W.T. Fedorko,¹³ R.G. Feild,⁵⁸
M. Feindt,²⁵ J.P. Fernandez,⁴⁶ R. Field,¹⁷ G. Flanagan,³⁴ L.R. Flores-Castillo,⁴⁵ A. Foland,²¹
S. Forrester,⁷ G.W. Foster,¹⁶ M. Franklin,²¹ J.C. Freeman,²⁸ Y. Fujii,²⁶ I. Furic,¹³ A. Gajjar,²⁹
M. Gallinaro,⁴⁸ J. Galyardt,¹² J.E. Garcia,⁴⁴ M. Garcia Sciveres,²⁸ A.F. Garfinkel,⁴⁶ C. Gay,⁵⁸
H. Gerberich,²³ E. Gerchtein,¹² D. Gerdes,³³ S. Giagu,⁴⁹ P. Giannetti,⁴⁴ A. Gibson,²⁸
K. Gibson,¹² C. Ginsburg,¹⁶ K. Giolo,⁴⁶ M. Giordani,⁵² M. Giunta,⁴⁴ G. Giurgiu,¹²

V. Glagolev,¹⁴ D. Glenzinski,¹⁶ M. Gold,³⁶ N. Goldschmidt,³³ J. Goldstein,⁴¹ G. Gomez,¹¹
G. Gomez-Ceballos,¹¹ M. Goncharov,⁵¹ O. González,⁴⁶ I. Gorelov,³⁶ A.T. Goshaw,¹⁵ Y. Gotra,⁴⁵
K. Goulianos,⁴⁸ A. Gresele,⁴² M. Griffiths,²⁹ S. Grinstein,²¹ C. Grosso-Pilcher,¹³ U. Grundler,²³
J. Guimaraes da Costa,²¹ C. Haber,²⁸ S.R. Hahn,¹⁶ K. Hahn,⁴³ E. Halkiadakis,⁴⁷ A. Hamilton,³²
B.-Y. Han,⁴⁷ R. Handler,⁵⁷ F. Happacher,¹⁸ K. Hara,⁵³ M. Hare,⁵⁴ S. Harper,⁴¹ R.F. Harr,⁵⁶
R.M. Harris,¹⁶ K. Hatakeyama,⁴⁸ J. Hauser,⁸ C. Hays,¹⁵ H. Hayward,²⁹ A. Heijboer,⁴³
B. Heinemann,²⁹ J. Heinrich,⁴³ M. Hennecke,²⁵ M. Herndon,⁵⁷ J. Heuser,²⁵ D. Hidas,¹⁵
C.S. Hill,¹⁰ D. Hirschbuehl,²⁵ A. Hocker,¹⁶ A. Holloway,²¹ S. Hou,¹ M. Houlden,²⁹ S.-C. Hsu,⁹
B.T. Huffman,⁴¹ R.E. Hughes,³⁸ J. Huston,³⁴ K. Ikado,⁵⁵ J. Incandela,¹⁰ G. Introzzi,⁴⁴ M. Iori,⁴⁹
Y. Ishizawa,⁵³ A. Ivanov,⁷ B. Iyutin,³¹ E. James,¹⁶ D. Jang,⁵⁰ B. Jayatilaka,³³ D. Jeans,⁴⁹
H. Jensen,¹⁶ E.J. Jeon,²⁷ M. Jones,⁴⁶ K.K. Joo,²⁷ S.Y. Jun,¹² T.R. Junk,²³ T. Kamon,⁵¹ J. Kang,³³
M. Karagoz-Unel,³⁷ P.E. Karchin,⁵⁶ Y. Kato,⁴⁰ Y. Kemp,²⁵ R. Kephart,¹⁶ U. Kerzel,²⁵
V. Khotilovich,⁵¹ B. Kilminster,³⁸ D.H. Kim,²⁷ H.S. Kim,²⁷ J.E. Kim,²⁷ M.J. Kim,¹² M.S. Kim,²⁷
S.B. Kim,²⁷ S.H. Kim,⁵³ Y.K. Kim,¹³ M. Kirby,¹⁵ L. Kirsch,⁶ S. Klimentenko,¹⁷ M. Klute,³¹
B. Knuteson,³¹ B.R. Ko,¹⁵ H. Kobayashi,⁵³ K. Kondo,⁵⁵ D.J. Kong,²⁷ J. Konigsberg,¹⁷
K. Kordas,¹⁸ A. Korytov,¹⁷ A.V. Kotwal,¹⁵ A. Kovalev,⁴³ J. Kraus,²³ I. Kravchenko,³¹ M. Kreps,²⁵
A. Kreymer,¹⁶ J. Kroll,⁴³ N. Krumnack,⁴ M. Kruse,¹⁵ V. Krutelyov,⁵¹ S. E. Kuhlmann,²
Y. Kusakabe,⁵⁵ S. Kwang,¹³ A.T. Laasanen,⁴⁶ S. Lai,³² S. Lami,⁴⁴ S. Lammel,¹⁶ M. Lancaster,³⁰
R.L. Lander,⁷ K. Lannon,³⁸ A. Lath,⁵⁰ G. Latino,⁴⁴ I. Lazzizzera,⁴² C. Lecci,²⁵ T. LeCompte,²
J. Lee,⁴⁷ J. Lee,²⁷ S.W. Lee,⁵¹ R. Lefèvre,³ N. Leonardo,³¹ S. Leone,⁴⁴ S. Levy,¹³ J.D. Lewis,¹⁶
K. Li,⁵⁸ C. Lin,⁵⁸ C.S. Lin,¹⁶ M. Lindgren,¹⁶ E. Lipeles,⁹ T.M. Liss,²³ A. Lister,¹⁹
D.O. Litvintsev,¹⁶ T. Liu,¹⁶ Y. Liu,¹⁹ N.S. Lockyer,⁴³ A. Loginov,³⁵ M. Loreti,⁴² P. Loverre,⁴⁹
R.-S. Lu,¹ D. Lucchesi,⁴² P. Lujan,²⁸ P. Lukens,¹⁶ G. Lungu,¹⁷ L. Lyons,⁴¹ J. Lys,²⁸ R. Lysak,¹
E. Lytken,⁴⁶ P. Mack,²⁵ D. MacQueen,³² R. Madrak,¹⁶ K. Maeshima,¹⁶ P. Maksimovic,²⁴
G. Manca,²⁹ F. Margaroli,⁵ R. Marginean,¹⁶ C. Marino,²³ A. Martin,⁵⁸ M. Martin,²⁴
V. Martin,³⁷ M. Martínez,³ T. Maruyama,⁵³ H. Matsunaga,⁵³ M.E. Mattson,⁵⁶ R. Mazini,³²
P. Mazzanti,⁵ K.S. McFarland,⁴⁷ D. McGivern,³⁰ P. McIntyre,⁵¹ P. McNamara,⁵⁰ R. McNulty,²⁹
A. Mehta,²⁹ S. Menzemer,³¹ A. Menzione,⁴⁴ P. Merkel,⁴⁶ C. Mesropian,⁴⁸ A. Messina,⁴⁹
M. von der Mey,⁸ T. Miao,¹⁶ N. Miladinovic,⁶ J. Miles,³¹ R. Miller,³⁴ J.S. Miller,³³ C. Mills,¹⁰
M. Milnik,²⁵ R. Miquel,²⁸ S. Miscetti,¹⁸ G. Mitselmakher,¹⁷ A. Miyamoto,²⁶ N. Moggi,⁵

B. Mohr,⁸ R. Moore,¹⁶ M. Morello,⁴⁴ P. Movilla Fernandez,²⁸ J. Mülmenstädt,²⁸ A. Mukherjee,¹⁶
 M. Mulhearn,³¹ Th. Muller,²⁵ R. Mumford,²⁴ P. Murat,¹⁶ J. Nachtman,¹⁶ S. Nahn,⁵⁸ I. Nakano,³⁹
 A. Napier,⁵⁴ D. Naumov,³⁶ V. Nacula,¹⁷ C. Neu,⁴³ M.S. Neubauer,⁹ J. Nielsen,²⁸ T. Nigmanov,⁴⁵
 L. Nodulman,² O. Norniella,³ T. Ogawa,⁵⁵ S.H. Oh,¹⁵ Y.D. Oh,²⁷ T. Okusawa,⁴⁰ R. Oldeman,²⁹
 R. Orava,²² K. Osterberg,²² C. Pagliarone,⁴⁴ E. Palencia,¹¹ R. Paoletti,⁴⁴ V. Papadimitriou,¹⁶
 A. Papikononou,²⁵ A.A. Paramonov,¹³ B. Parks,³⁸ S. Pashapour,³² J. Patrick,¹⁶ G. Pauletta,⁵²
 M. Paulini,¹² C. Paus,³¹ D.E. Pellett,⁷ A. Penzo,⁵² T.J. Phillips,¹⁵ G. Piacentino,⁴⁴ J. Piedra,¹¹
 K. Pitts,²³ C. Plager,⁸ L. Pondrom,⁵⁷ G. Pope,⁴⁵ X. Portell,³ O. Poukhov,¹⁴ N. Pounder,⁴¹
 F. Prakoshyn,¹⁴ A. Pronko,¹⁶ J. Proudfoot,² F. Ptohos,¹⁸ G. Punzi,⁴⁴ J. Pursley,²⁴ J. Rademacker,⁴¹
 A. Rahaman,⁴⁵ A. Rakitin,³¹ S. Rappoccio,²¹ F. Ratnikov,⁵⁰ B. Reiser,¹⁶ V. Rekovic,³⁶
 N. van Remortel,²² P. Renton,⁴¹ M. Rescigno,⁴⁹ S. Richter,²⁵ F. Rimondi,⁵ K. Rinnert,²⁵
 L. Ristori,⁴⁴ W.J. Robertson,¹⁵ A. Robson,²⁰ T. Rodrigo,¹¹ E. Rogers,²³ S. Rolli,⁵⁴ R. Roser,¹⁶
 M. Rossi,⁵² R. Rossin,¹⁷ C. Rott,⁴⁶ A. Ruiz,¹¹ J. Russ,¹² V. Rusu,¹³ D. Ryan,⁵⁴ H. Saarikko,²²
 S. Sabik,³² A. Safonov,⁷ W.K. Sakumoto,⁴⁷ G. Salamanna,⁴⁹ O. Salto,³ D. Saltzberg,⁸
 C. Sanchez,³ L. Santi,⁵² S. Sarkar,⁴⁹ K. Sato,⁵³ P. Savard,³² A. Savoy-Navarro,¹⁶ T. Scheidle,²⁵
 P. Schlabach,¹⁶ E.E. Schmidt,¹⁶ M.P. Schmidt,⁵⁸ M. Schmitt,³⁷ T. Schwarz,³³ L. Scodellaro,¹¹
 A.L. Scott,¹⁰ A. Scribano,⁴⁴ F. Scuri,⁴⁴ A. Sedov,⁴⁶ S. Seidel,³⁶ Y. Seiya,⁴⁰ A. Semenov,¹⁴
 F. Semeria,⁵ L. Sexton-Kennedy,¹⁶ I. Sfiligoi,¹⁸ M.D. Shapiro,²⁸ T. Shears,²⁹ P.F. Shepard,⁴⁵
 D. Sherman,²¹ M. Shimojima,⁵³ M. Shochet,¹³ Y. Shon,⁵⁷ I. Shreyber,³⁵ A. Sidoti,⁴⁴ A. Sill,¹⁶
 P. Sinervo,³² A. Sisakyan,¹⁴ J. Sjolín,⁴¹ A. Skiba,²⁵ A.J. Slaughter,¹⁶ K. Sliwa,⁵⁴ D. Smirnov,³⁶
 J. R. Smith,⁷ F.D. Snider,¹⁶ R. Snihur,³² M. Soderberg,³³ A. Soha,⁷ S. Somalwar,⁵⁰ V. Sorin,³⁴
 J. Spalding,¹⁶ F. Spinella,⁴⁴ P. Squillacioti,⁴⁴ M. Stanitzki,⁵⁸ A. Staveris-Polykalas,⁴⁴
 R. St. Denis,²⁰ B. Stelzer,⁸ O. Stelzer-Chilton,³² D. Stentz,³⁷ J. Strologas,³⁶ D. Stuart,¹⁰ J.S. Suh,²⁷
 A. Sukhanov,¹⁷ K. Sumorok,³¹ H. Sun,⁵⁴ T. Suzuki,⁵³ A. Taffard,²³ R. Tafirout,³² R. Takashima,³⁹
 Y. Takeuchi,⁵³ K. Takikawa,⁵³ M. Tanaka,² R. Tanaka,³⁹ M. Tecchio,³³ P.K. Teng,¹ K. Terashi,⁴⁸
 S. Tether,³¹ J. Thom,¹⁶ A.S. Thompson,²⁰ E. Thomson,⁴³ P. Tipton,⁴⁷ V. Tiwari,¹² S. Tkaczyk,¹⁶
 D. Toback,⁵¹ K. Tollefson,³⁴ T. Tomura,⁵³ D. Tonelli,⁴⁴ M. Tönnemann,³⁴ S. Torre,⁴⁴
 D. Torretta,¹⁶ S. Tourneur,¹⁶ W. Trischuk,³² R. Tsuchiya,⁵⁵ S. Tsuno,³⁹ N. Turini,⁴⁴ F. Ukegawa,⁵³
 T. Unverhau,²⁰ S. Uozumi,⁵³ D. Usynin,⁴³ L. Vacavant,²⁸ A. Vaiciulis,⁴⁷ S. Vallecorsa,¹⁹
 A. Varganov,³³ E. Vataga,³⁶ G. Velez,¹⁶ G. Veramendi,²³ V. Veszpremi,⁴⁶ T. Vickey,²³ R. Vidal,¹⁶

I. Vila,¹¹ R. Vilar,¹¹ I. Vollrath,³² I. Volobouev,²⁸ F. Würthwein,⁹ P. Wagner,⁵¹ R. G. Wagner,²
R.L. Wagner,¹⁶ W. Wagner,²⁵ R. Wallny,⁸ T. Walter,²⁵ Z. Wan,⁵⁰ M.J. Wang,¹ S.M. Wang,¹⁷
A. Warburton,³² B. Ward,²⁰ S. Waschke,²⁰ D. Waters,³⁰ T. Watts,⁵⁰ M. Weber,²⁸ W.C. Wester III,¹⁶
B. Whitehouse,⁵⁴ D. Whiteson,⁴³ A.B. Wicklund,² E. Wicklund,¹⁶ H.H. Williams,⁴³
P. Wilson,¹⁶ B.L. Winer,³⁸ P. Wittich,⁴³ S. Wolbers,¹⁶ C. Wolfe,¹³ S. Worm,⁵⁰ T. Wright,³³
X. Wu,¹⁹ S.M. Wynne,²⁹ A. Yagil,¹⁶ K. Yamamoto,⁴⁰ J. Yamaoka,⁵⁰ Y. Yamashita,³⁹ C. Yang,⁵⁸
U.K. Yang,¹³ W.M. Yao,²⁸ G.P. Yeh,¹⁶ J. Yoh,¹⁶ K. Yorita,¹³ T. Yoshida,⁴⁰ I. Yu,²⁷ S.S. Yu,⁴³
J.C. Yun,¹⁶ L. Zanello,⁴⁹ A. Zanello,⁵² I. Zaw,²¹ F. Zetti,⁴⁴ X. Zhang,²³ J. Zhou,⁵⁰ and S. Zucchelli⁵

(CDF Collaboration)

¹*Institute of Physics, Academia Sinica,
Taipei, Taiwan 11529, Republic of China*

²*Argonne National Laboratory, Argonne, Illinois 60439*

³*Institut de Física d'Altes Energies, Universitat Autònoma de Barcelona,
E-08193, Bellaterra (Barcelona), Spain*

⁴*Baylor University, Waco, Texas 76798*

⁵*Istituto Nazionale di Fisica Nucleare,
University of Bologna, I-40127 Bologna, Italy*

⁶*Brandeis University, Waltham, Massachusetts 02254*

⁷*University of California, Davis, Davis, California 95616*

⁸*University of California, Los Angeles, Los Angeles, California 90024*

⁹*University of California, San Diego, La Jolla, California 92093*

¹⁰*University of California, Santa Barbara, Santa Barbara, California 93106*

¹¹*Instituto de Física de Cantabria, CSIC-University of Cantabria, 39005 Santander, Spain*

¹²*Carnegie Mellon University, Pittsburgh, PA 15213*

¹³*Enrico Fermi Institute, University of Chicago, Chicago, Illinois 60637*

¹⁴*Joint Institute for Nuclear Research, RU-141980 Dubna, Russia*

¹⁵*Duke University, Durham, North Carolina 27708*

¹⁶*Fermi National Accelerator Laboratory, Batavia, Illinois 60510*

¹⁷*University of Florida, Gainesville, Florida 32611*

¹⁸*Laboratori Nazionali di Frascati, Istituto Nazionale di Fisica Nucleare, I-00044 Frascati, Italy*

¹⁹*University of Geneva, CH-1211 Geneva 4, Switzerland*

- ²⁰*Glasgow University, Glasgow G12 8QQ, United Kingdom*
- ²¹*Harvard University, Cambridge, Massachusetts 02138*
- ²²*Division of High Energy Physics, Department of Physics,
University of Helsinki and Helsinki Institute of Physics, FIN-00014, Helsinki, Finland*
- ²³*University of Illinois, Urbana, Illinois 61801*
- ²⁴*The Johns Hopkins University, Baltimore, Maryland 21218*
- ²⁵*Institut für Experimentelle Kernphysik,
Universität Karlsruhe, 76128 Karlsruhe, Germany*
- ²⁶*High Energy Accelerator Research Organization (KEK), Tsukuba, Ibaraki 305, Japan*
- ²⁷*Center for High Energy Physics: Kyungpook National University,
Taegu 702-701; Seoul National University,
Seoul 151-742; and SungKyunKwan University, Suwon 440-746; Korea*
- ²⁸*Ernest Orlando Lawrence Berkeley National Laboratory, Berkeley, California 94720*
- ²⁹*University of Liverpool, Liverpool L69 7ZE, United Kingdom*
- ³⁰*University College London, London WC1E 6BT, United Kingdom*
- ³¹*Massachusetts Institute of Technology, Cambridge, Massachusetts 02139*
- ³²*Institute of Particle Physics: McGill University, Montréal,
Canada H3A 2T8; and University of Toronto, Toronto, Canada M5S 1A7*
- ³³*University of Michigan, Ann Arbor, Michigan 48109*
- ³⁴*Michigan State University, East Lansing, Michigan 48824*
- ³⁵*Institution for Theoretical and Experimental Physics, ITEP, Moscow 117259, Russia*
- ³⁶*University of New Mexico, Albuquerque, New Mexico 87131*
- ³⁷*Northwestern University, Evanston, Illinois 60208*
- ³⁸*The Ohio State University, Columbus, Ohio 43210*
- ³⁹*Okayama University, Okayama 700-8530, Japan*
- ⁴⁰*Osaka City University, Osaka 588, Japan*
- ⁴¹*University of Oxford, Oxford OX1 3RH, United Kingdom*
- ⁴²*University of Padova, Istituto Nazionale di Fisica Nucleare,
Sezione di Padova-Trento, I-35131 Padova, Italy*
- ⁴³*University of Pennsylvania, Philadelphia, Pennsylvania 19104*
- ⁴⁴*Istituto Nazionale di Fisica Nucleare Pisa, Universities of Pisa,
Siena and Scuola Normale Superiore, I-56127 Pisa, Italy*

⁴⁵*University of Pittsburgh, Pittsburgh, Pennsylvania 15260*

⁴⁶*Purdue University, West Lafayette, Indiana 47907*

⁴⁷*University of Rochester, Rochester, New York 14627*

⁴⁸*The Rockefeller University, New York, New York 10021*

⁴⁹*Istituto Nazionale di Fisica Nucleare, Sezione di Roma 1,*

University of Rome “La Sapienza,” I-00185 Roma, Italy

⁵⁰*Rutgers University, Piscataway, New Jersey 08855*

⁵¹*Texas A&M University, College Station, Texas 77843*

⁵²*Istituto Nazionale di Fisica Nucleare, University of Trieste/ Udine, Italy*

⁵³*University of Tsukuba, Tsukuba, Ibaraki 305, Japan*

⁵⁴*Tufts University, Medford, Massachusetts 02155*

⁵⁵*Waseda University, Tokyo 169, Japan*

⁵⁶*Wayne State University, Detroit, Michigan 48201*

⁵⁷*University of Wisconsin, Madison, Wisconsin 53706*

⁵⁸*Yale University, New Haven, Connecticut 06520*

(Dated: October 11, 2005)

Abstract

We present a search for $t\bar{t}$ events with a tau lepton in the final state. The data sample corresponds to an integrated luminosity of 194 pb^{-1} collected with the CDF II detector from $p\bar{p}$ collisions at a center of mass energy of 1.96 TeV. We observe two events with an expected signal of 1.0 ± 0.2 events and a background of 1.3 ± 0.3 events. We determine a 95% confidence level upper limit on r_τ , the ratio of the measured rate of $t \rightarrow \tau\nu q$ to the expectation, of 5.2.

PACS numbers: 14.65.Ha, 14.60.Fg

An experimental investigation of the interactions among the massive fermions of the third generation - the top and bottom quarks, the tau lepton and tau neutrino - has the potential to yield powerful insights into the puzzles of flavor and fermion mass. There is no adequate explanation for the comparatively large masses of the third generation particles [1], and we do not understand why there appear to be three and only three generations. A significant deviation in the number of observed $t \rightarrow \tau\nu q$ candidates from the rate predicted by the standard model could indicate an anomalous coupling among the third generation particles. Extensions of the standard model could lead to alternative modes of top quark decay that enhance the top branching fraction to this final state. One example is the Minimal Supersymmetric Standard Model [2–4], where the top quark could decay into a b -quark and a charged Higgs boson with subsequent decay into a tau lepton and tau neutrino. Other possibilities include R -parity violating SUSY decays of top [5] and new Z' bosons with non-generation universal couplings [6].

In this letter, we search for $t \rightarrow \tau\nu q$ decays in $194 \pm 11 \text{ pb}^{-1}$ of $p\bar{p}$ collisions collected by the CDF collaboration at the $\sqrt{s} = 1.96 \text{ TeV}$ Tevatron collider at Fermilab. The top quark, discovered at Fermilab by the CDF and DØ experiments in 1995 [7, 8], is predominantly produced via pair production, where the next to leading order quantum chromodynamics (QCD) theoretical prediction [9, 10] for the cross section is $6.7_{-0.9}^{+0.7} \text{ pb}$. In the standard model, the top quark is expected to decay with a branching fraction of almost 100% into a W boson and a b -quark. The branching fraction for the decay of a W boson to $\tau\nu$ is measured to be $10.74 \pm 0.27 \%$ [1]. Using the procedure described in this letter we interpret the results of the only previous search for $t \rightarrow \tau\nu q$ in $t\bar{t}$ production [11] to exclude anomalous rates above 18 times that expected in the standard model at 95% confidence level.

In this search, we select $t\bar{t}$ candidates where one top decays to $\tau\nu b$, and identify the tau lepton by its semi-hadronic decay. We do not search for tau lepton decays to electrons and muons, as these are difficult to distinguish from electrons and muons directly from W boson decay. We require the other top to decay to either $e\nu b$ or to $\mu\nu b$ in order to utilize the efficient high p_T [12] electron/muon triggers and to reduce the background from multi-jet production. We require significant missing transverse energy from the neutrinos, and at least two jets with high E_T [12], though we make no requirement on the heavy flavor content of the jets. Finally, we apply several novel kinematic and topological requirements designed to reject specific backgrounds.

The data used for this analysis were collected by the CDF Collaboration from March 2002 to September 2003. The CDF II detector [13] is an azimuthally and forward-backward symmetric

apparatus built to study the physics of $p\bar{p}$ collisions at \sqrt{s} of 1.96 TeV. The detector contains a charged-particle tracking system inside a 1.4 T field generated by a solenoid coaxial with the p and \bar{p} beams. A silicon microstrip detector provides track measurements between 1.5 and 28 cm in radius from the beam axis for charged particles with pseudorapidity, $|\eta| < 2$ [12]. A 3.1 m long open cell drift chamber measures track position at 96 points at radii between 40 and 137 cm for particles with $|\eta| < 1$.

Segmented electromagnetic and hadronic sampling calorimeters surround the tracking volume and cover the range $|\eta| < 3.6$. The central ($|\eta| \lesssim 1$) calorimeters, in which τ decays are identified in this analysis, are divided into towers with segmentation in azimuthal angle of 15 degrees and in pseudorapidity of about 0.1. The central electron shower detector (CES) consists of proportional chambers with wires and cathode strips arranged orthogonally with pitch varying from 1.4 to 2.0 cm located at a depth of 6 radiation lengths within the electromagnetic calorimeter, at the position where the lateral profile of the shower is maximum. This fine segmentation of the CES measures electromagnetic shower position with ≈ 3 mm resolution and allows reconstruction of the boosted $\pi^0 \rightarrow \gamma\gamma$ produced in tau decays. A set of drift chambers located outside the hadron calorimeters and a second set outside a 60 cm iron shield detect muon candidates with $|\eta| < 0.6$. Additional chambers and scintillator counters extend this muon coverage in $0.6 < |\eta| < 1.0$ for most azimuthal angles. The luminosity is determined to an accuracy of 6% using gas Cherenkov counters covering $3.7 < |\eta| < 4.7$ which measure the average number of inelastic $p\bar{p}$ collisions per bunch crossing.

The CDF triggers used in this analysis select samples with at least one high p_T central electron or muon candidate. The electron trigger requires candidates to have E_T greater than 18 GeV, and the muon trigger requires a candidate with $p_T > 18$ GeV/c [14]. Further identification requirements are placed to select a pure sample of electrons and muons and are described in detail elsewhere [15, 16]. Neutrinos escape the calorimeter undetected and result in missing transverse energy (\cancel{E}_T) which is measured by balancing the calorimeter energy in the transverse plane. We require $\cancel{E}_T > 20$ GeV after corrections for identified muons.

Semi-hadronic decays of taus produced in W decay have a distinctive signature of narrow, isolated jets with low charged track multiplicity. The calorimeter measures the visible energy of the tau jet, while the central tracker and CES determine the narrowness and multiplicity. A tau candidate requires a tau calorimeter cluster and a COT track with a minimum p_T of 4.5 GeV/c pointing to the cluster. A tau calorimeter cluster requires a tower with $E_T \geq 6$ GeV and no more

than five adjacent towers with $E_T > 1$ GeV.

After lepton candidate selection, we impose additional requirements on the isolation of the tau lepton to reduce backgrounds from jets. A cone is formed around the seed track with a variable angular radius, $\theta_{\text{cone}} = \text{Min}\{0.17, (5 \text{ GeV})/E_{\text{tau cluster}}\}$ rad. The tau candidate is required to have one or three tracks in the signal cone to be consistent with the dominant decay modes of the tau. If there are three tracks the sum of the electric charges must be equal to ± 1 . Candidate π^0 s are identified in the calorimeter from clusters of energy observed in the CES. The tau p_T is estimated to be the sum of the seed track p_T plus the sum of the π^0 E_T/c . The tau p_T is required to be greater than 15 GeV/c, and the invariant mass of the π^0 s and the tracks is required to be less than 1.8 GeV to be consistent with the mass of the tau. An isolation annulus is defined around the tau cone extending from the cone edge, θ_{cone} , to 0.52 radians in which no tracks or π^0 candidates may be present. Calorimeter towers within the isolation annulus are required to have E_T less than 6% of the tau E_T . Additional requirements are imposed to reject tau candidates that resemble electrons or muons based on track and calorimeter characteristics. To remove electrons, the energy in the hadronic calorimeter divided by the track momentum sum of the tau candidate, $E_{\text{had}}/\sum p$, is required to be greater than 0.15. To remove muons, the E_T of the calorimeter cluster energy associated with the tau candidate divided by the p_T of the seed track, E_T/p_T , is required to be greater than 0.5. The combined tau identification and isolation efficiency is 35%.

In addition to the electron or muon, the tau candidate and the missing transverse energy, we require at least two jets, corresponding to the expected number of b quarks produced in the $t\bar{t}$ decays. We require that these jets have $|\eta| < 2$ and that the first and second highest jets have E_T greater than 25 GeV and 15 GeV, respectively. The event H_T , defined as the scalar sum of the electron E_T or muon p_T , the tau p_T , the \cancel{E}_T and the E_T of the jets, must exceed 205 GeV. These jet and H_T requirements reduce the backgrounds from W bosons produced in association with jets by $\approx 85\%$, while removing only $\approx 5\%$ of the $t\bar{t}$ signal.

We determine the efficiency of the selection cuts by simulating standard model $t\bar{t}$ detection with the PYTHIA [17] event generator, the TAUOLA [18] tau decay simulation and a GEANT-based model [19] of the CDF detector and trigger response. We independently determine the electron, muon and tau identification and trigger efficiencies. Electron and muon efficiencies are determined using $Z \rightarrow e^+e^-$ and $Z \rightarrow \mu^+\mu^-$ events respectively with one of the electrons (muons) required to pass tight identification cuts and the other electron (muon) used to determine the efficiency. The tau identification efficiency is determined by comparing numbers of observed $W \rightarrow \tau\nu$ to

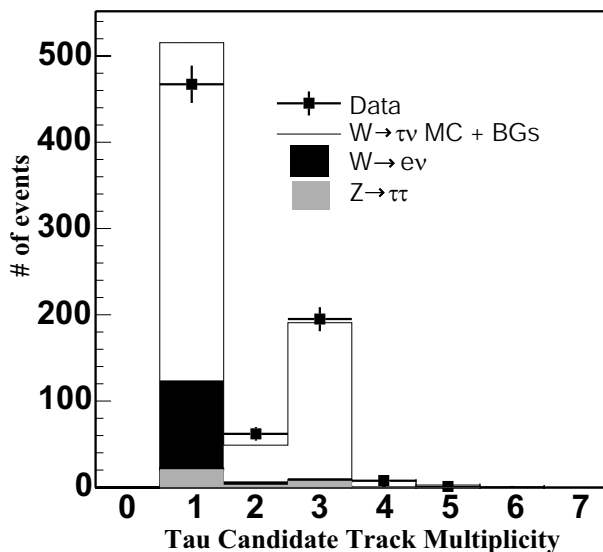


FIG. 1: The number of tracks in the reconstructed tau in $W \rightarrow \tau\nu$ candidates

the prediction of the simulation. Where there are differences between the data and the simulation, we derive correction factors ($< 5\%$ in most cases) which are applied to results of the simulation. Figure 1 compares the distribution of the number of tracks in the tau cone for $W \rightarrow \tau\nu$ candidates to the simulation with the addition of expected backgrounds from $W \rightarrow e\nu$, determined from the data, and $Z \rightarrow \tau\tau$, determined from Monte Carlo. In the case of tau identification, we find that the ratio of the efficiency in data to that in simulation is 0.90 ± 0.06 . In addition to contributions from the uncertainty in lepton identification efficiency, there are significant uncertainties from the modeling of the jet energy response in the calorimeter and in the simulation of initial and final state QCD radiation. Table I summarizes the systematic uncertainties in the efficiency for detecting the signal process.

Our dominant background is W bosons produced in association with jets, where the W decays to $e\nu$ or $\mu\nu$ and one of the jets is misidentified as a tau. We determine the number of such events we expect from the data. We first find a sample of relaxed tau candidates passing all tau identification requirements except the isolation, mass and track quality requirements. This sample is dominated by jets rather than tau leptons. To that sample, we apply a relative fake rate, which is the probability that those relaxed tau candidates will pass all identification requirements. The relative fake rate of jets to identified tau candidates is measured in four independent jet data samples; three of the samples were selected with different jet E_T threshold requirements and the fourth sample was

Source	signal prediction uncertainty
Jet Energy Scale	$\pm 6\%$
Electron and Muon Identification	$\pm 5\%$
Tau Identification	$\pm 6\%$
Top Production Model	$\pm 7\%$
Initial State Radiation	$\pm 7\%$
Final State Radiation	$\pm 7\%$
Parton Distribution Functions	$\pm 1\%$
Total	$\pm 16\%$

TABLE I: Summary of systematic uncertainties in the identification of $t\bar{t}$ (signal) events

selected using a requirement on the sum of the E_T of all calorimeter towers in the event. The relative fake rate is parameterized as a function of jet E_T and isolation of the jet in the calorimeter. The full spread in the measured fake rates of the four different samples is 26%, which we take as our estimate of the systematic uncertainty in this procedure.

Events with electrons or muons that fake tau candidates are another significant background source. These events originate primarily from the production of Z bosons, decaying to e^+e^- or $\mu^+\mu^-$, in association with extra jets. In the case of electrons, the event can be a background when the electron energy is poorly reconstructed; in the case of muons, a muon can fake a tau if the muon suffers a catastrophic energy loss in the calorimeter. To estimate the electron background, we first measure an electron to tau fake rate using $Z \rightarrow e^+e^-$ events. We then scale the number of events with tau candidates that fail the electron rejection requirement but pass all other analysis requirements by the electron to tau fake rate. An ALPGEN [20] interfaced with HERWIG [21] simulation of $Z \rightarrow \mu^+\mu^-$ events with extra jets is used to predict the muon background, and we confirm the modeling of the muon energy response in the calorimeter using $Z \rightarrow \mu^+\mu^-$ events in the data.

Figure 2 shows evidence of fake tau background from jets and electrons in the electron + tau candidate data with relaxed tau identification requirements. The tau contribution to the region shown outside of the signal requirements is expected to be a small fraction of that inside.

Another class of background events results from processes other than $t\bar{t}$ production that create tau leptons in association with electrons or muons. The largest of these backgrounds is from Z

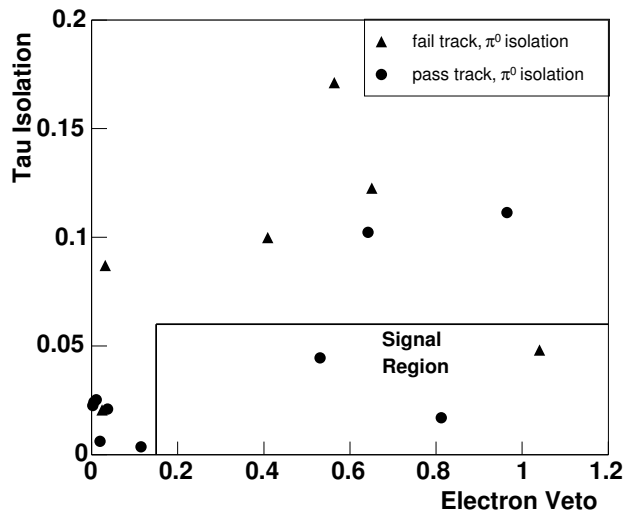


FIG. 2: Evidence for fake tau background. For events with a tau candidate, an electron, \cancel{E}_T and two jets, we show the ratio of energy in the tau calorimeter isolation cone divided by tau p_T (“tau isolation”) vs. the “electron veto” variable, the energy in the hadronic calorimeter divided by the track momentum sum of the tau candidate, $E_{had}/\sum p$. Events with fake tau candidates from jets are at high tau isolation; di-electron events appear at low isolation and low $E_{had}/\sum p$. The analysis requirements are shown by lines on the plots. The triangular markers identify events which fail the tau identification requirements of no π^0 s and tracks in the isolation annulus.

boson production in association with jets where $Z \rightarrow \tau^+\tau^-$ with one fully leptonic and one semi-hadronic tau decay. In this process, the energy spectra of the leptons, jets and the \cancel{E}_T are softer than the predictions from $t\bar{t}$ production. As a result, our H_T requirement reduces this background by about 40%. However, even with such a requirement the previous search for this decay chain at CDF [11] predicted a higher number of $Z \rightarrow \tau^+\tau^-$ background events than $t\bar{t}$ signal events. Therefore, we developed a selection that targets this background exclusively. $Z \rightarrow \tau^+\tau^-$ decays that pass the H_T and \cancel{E}_T requirements have a Z boson with significant p_T . In these events, one can reconstruct the Z mass from the observed tau decay products by assuming that the \cancel{E}_T in the events results entirely from neutrinos produced in τ decays and that those neutrinos are collinear with the other τ decay products. In this case, there is a unique assignment of the energy of unobserved neutrinos from each tau candidate based on the direction of the \cancel{E}_T . For there to be a sensible solution, the \cancel{E}_T must be able to be decomposed into components parallel to the direction of both the electron or muon and the tau candidate, i.e. the \cancel{E}_T must point in a direction between the

Process	Number of expected events
$\gamma^*/Z \rightarrow \tau\tau + \text{jets}$	$0.25 \pm 0.06 \pm 0.05$
$W/Z + \text{jets with jet} \rightarrow \tau \text{ fake}$	$0.75 \pm 0.12 \pm 0.20$
$\gamma^*/Z \rightarrow ee + \text{jets with } e \rightarrow \tau \text{ fake}$	$0.08 \pm 0.03 \pm 0.02$
$\gamma^*/Z \rightarrow \mu\mu + \text{jets with } \mu \rightarrow \tau \text{ fake}$	$0.05 \pm 0.03 \pm 0.01$
WW	$0.14 \pm 0.02 \pm 0.03$
WZ	$0.02 \pm 0.02 \pm 0.01$
Total expected background events	$1.29 \pm 0.14 \pm 0.21$
Expected signal	$1.00 \pm 0.06 \pm 0.16$

TABLE II: Summary of background and signal predictions. The first error is from simulation statistics, and the second is from systematic uncertainties. The expected signal assumes a $t\bar{t}$ cross-section of 6.7 pb.

transverse momenta of the electron or muon and the tau candidate. For $t\bar{t}$ events, this is most often not the case, and the assignment of \cancel{E}_T to a neutrino would result in the neutrino carrying negative momentum from the tau decay. For events where this reconstruction is possible, we remove events in a window around the Z mass. This results in an additional 88% reduction of $Z \rightarrow \tau^+\tau^-$ events while removing only 4% of $t\bar{t}$ signal.

The other physics processes that can reproduce the final state with taus are WW and WZ bosons created in association with jets. The product of the theoretical cross-section and branching ratios for these processes is much smaller than that of $t\bar{t}$, and they are also removed preferentially by the H_T requirement. We predict the background based on a simulation of diboson production from the HERWIG generator [21]. An additional source of $t \rightarrow \tau\nu q$ signal events in electroweak single top production is expected to contribute fewer than 0.01 events. We summarize all backgrounds in Table II.

We use an independent control sample to test our calculation of backgrounds. The selection of the electrons, muons, taus and \cancel{E}_T is identical to our signal selection, but the number of jets in the sample is restricted to be less than two. Also, in order to increase the statistics for this comparison we do not impose the H_T requirement or the Z mass removal on these events. Table III shows the comparisons of predicted and observed events. We categorize the results based on jet multiplicity, electron or muon final state, and the cases of the same or opposite charge in the two leptons.

The data in Table III can be used as a control experiment to check the accuracy of our back-

channel	# jets	predicted # events	measured # events
e + τ opp sign	0	23.7 \pm 3.6	17
e + τ opp sign	1	4.6 \pm 0.9	5
e + τ same sign	0	7.3 \pm 1.8	8
e + τ same sign	1	1.9 \pm 0.6	3
μ + τ opp sign	0	21.3 \pm 3.3	11
μ + τ opp sign	1	2.7 \pm 0.6	4
μ + τ same sign	0	5.6 \pm 1.5	3
μ + τ same sign	1	0.8 \pm 0.3	0

TABLE III: Comparison between the predicted and measured number of events for low jet multiplicities

	Candidate #1	Candidate #2
tau p_T (GeV/c)	39	20
electron p_T (GeV/c)	40	79
# of tau tracks	1	3
H_T (GeV)	286	239
Number of jets	3	2
jet1 E_T (GeV)	73 †	35
jet2 E_T (GeV)	40	34
jet3 E_T (GeV)	35	n/a
\cancel{E}_T (GeV)	59	72

TABLE IV: Properties of the candidate events. The jet marked with the † is tagged as a b by the presence of a secondary vertex [22].

ground predictions. *A priori*, we chose as the statistic of the control experiment the joint probability of the observed number of events given the prediction for the eight samples in this table. The expected distribution of these joint probabilities is measured via simulated pseudo-experiments which account for the uncertainties in the predictions and the Poisson fluctuations from the limited statistics in the data. We find the data in Table III have a joint probability which is higher than 41% of our pseudo-experiments and conclude that this control data are consistent with our expected background predictions.

The theoretical $t\bar{t}$ production cross-section is $6.7_{-0.9}^{+0.7}$ pb [9, 10] for a top quark mass of $175 \text{ GeV}/c^2$, and the acceptance, including all branching fractions in the decay channel, is $0.076 \pm 0.005(\text{stat.}) \pm 0.013(\text{syst.})\%$. For a $t\bar{t}$ cross-section of 6.7 pb we therefore expect 1.00 ± 0.17 signal events in 194 pb^{-1} , in addition to the background expectation of 1.29 ± 0.25 events. We observe 2 events. Both events are in the electron + tau channel, and properties of these two events are listed in Table IV.

We define the ratio

$$r_\tau \equiv \frac{\Gamma(t \rightarrow \tau\nu q)}{\Gamma_{SM}(t \rightarrow \tau\nu q)}$$

as a measure of a possible anomalous enhancement in the rate. Using the method of Rolke *et alia* [23], we set an upper limit on r_τ of 5.2 at the 95% confidence level. The previous result from CDF Run I [11] would yield a limit of $r_\tau < 18$ at the 95% confidence level using the same statistical methods.

In summary, we have searched for top decay into $\tau\nu q$ by identifying semi-hadronic decays of tau leptons in $t\bar{t}$ events. We observe two candidate events, consistent with the standard model, and set an upper limit on the ratio of observed production of $t \rightarrow \tau\nu q$ to the standard model expectation.

Acknowledgments

We thank the Fermilab staff and the technical staffs of the participating institutions for their vital contributions. This work was supported by the U.S. Department of Energy and National Science Foundation; the Italian Istituto Nazionale di Fisica Nucleare; the Ministry of Education, Culture, Sports, Science and Technology of Japan; the Natural Sciences and Engineering Research Council of Canada; the National Science Council of the Republic of China; the Swiss National Science Foundation; the A.P. Sloan Foundation; the Research Corporation; the Bundesministerium für Bildung und Forschung, Germany; the Korean Science and Engineering Foundation and the Korean Research Foundation; the Particle Physics and Astronomy Research Council and the Royal Society, UK; the Russian Foundation for Basic Research; the Comisión Interministerial de Ciencia y Tecnología, Spain; in part by the European Community's Human Potential Programme under

contract HPRN-CT-2002-00292; and the Academy of Finland.

- [1] Particle Data Group, Phys. Lett. **B592**, 1 (2004).
- [2] V. Barger and R.J.N. Phillips, Phys. Rev. **D41**, 884 (1990).
- [3] J. Guasch and J. Sola, Phys. Lett. **B416**, 353 (1998).
- [4] T. Affolder *et al.* [CDF collaboration], Phys. Rev. **D62**, 012004 (2000).
- [5] T. Han and M.B. Magro, Phys. Lett. **B476**, 79 (2000).
- [6] C. Yue, H. Zong and L. Liu, Mod. Phys. Lett. **A18**, 2187 (2003).
- [7] F. Abe *et al.* [CDF collaboration], Phys. Rev. Lett. **74**, 2626 (1995).
- [8] S. Abachi *et al.* [DØ collaboration], Phys. Rev. Lett. **74**, 2632 (1995).
- [9] M. Cacciari, S. Frixione, M. L. Mangano, P. Nason and G. Ridolfi, JHEP **0404**, 068 (2004).
- [10] N. Kidonakis and R. Vogt, Phys. Rev. **D68**, 114014 (2003).
- [11] F. Abe *et al.* [CDF collaboration], Phys. Rev. Lett. **79**, 3585 (1997).
- [12] CDF uses a cylindrical coordinate system in which ϕ is the azimuthal angle, r is the radius from the nominal beamline, and $+z$ points in the direction of the proton beam and is zero at the center of the detector. The pseudorapidity $\eta = -\ln[\tan(\theta/2)]$, where θ is the polar angle with respect to the z axis. Calorimeter energy (track momentum) measured transverse to the beam is denoted as E_T (p_T). Track p_T is evaluated from its curvature assuming a singly-charged particle, and is half of the true p_T for a doubly-charged particle.
- [13] D. Acosta, *et al.* [CDF collaboration], Phys. Rev. **D71**, 032001 (2005).
- [14] D. Acosta *et al.* [CDF collaboration], Phys. Rev. **D71**, 072005 (2005).
- [15] D. Acosta *et al.* [CDF collaboration], arXiv:hep-ex/0406078, submitted to Phys. Rev. Lett.
- [16] D. Acosta *et al.* [CDF collaboration], Phys. Rev. Lett. **93**, 142001 (2004).
- [17] T. Sjostrand, Comput. Phys. Commun. **82**, 74 (1994).
- [18] S. Jadach *et al.*, CERN-TH-6793 (1992).
- [19] S. Agostinelli *et al.* [GEANT4 collaboration], Nucl. Inst. Meth. **A506** 250 (2003).
- [20] M. Mangano, *et al.*, JHEP **07**, 001 (2003).
- [21] G. Corcella, *et al.*, JHEP **0101**, 010 (2001).
- [22] D. Acosta *et al.* [CDF collaboration], FERMILAB-PUB-04-275-E, arXiv:hep-ex/0410041, submitted to Phys. Rev. **D**.

[23] W. A. Rolke, A. M. Lopez, and J. Conrad, arXiv:physics/0403059.